

# Higgs exclusion and the $H \rightarrow WW^* \rightarrow l\nu c j$ semi-leptonic channel at the Tevatron

Arjun Menon

*Illinois Institute of Technology, Chicago, Illinois 60616-3793, USA and  
Department of Physics, University of Oregon, Eugene, OR 97403, USA*

Zack Sullivan\*

*Illinois Institute of Technology, Chicago, Illinois 60616-3793, USA*

(Dated: September 29, 2011)

We study the Higgs boson decay to  $W^+W^-$ , where one boson decays to leptons, and the other decays to  $c$ +jet at Tevatron. Given the current charm tagging acceptances, this channel can help improve and confirm the current combined Tevatron exclusion limit on a standard model-like Higgs boson. If charm acceptance can be improved to at least 24%, this channel could provide the second tightest limits on a Higgs boson mass between 140–190 GeV from a single channel measurement.

PACS numbers: 14.80.Bn, 13.85.Qk, 13.38.-b, 13.85.Ni

## I. INTRODUCTION

As data collection concludes at the Fermilab Tevatron, the CDF and DØ experiments are combining their results to place strong constraints on the existence of a standard model-like Higgs boson [1]. The strongest constraints come from the search for  $H \rightarrow WW \rightarrow l^+l^-\nu\bar{\nu}$  [2–4], setting preliminary Tevatron mass exclusion limit of 156–177 GeV [1, 5, 6]. Several other modes have also been measured in order to contribute to this limit [7, 8], but have significantly less reach. In this paper we propose that the Tevatron experiments add the channel  $H \rightarrow l\nu c j$  to the final combination limit. We first proposed in Ref. [9]  $H \rightarrow l\nu c j$  for analysis at the CERN Large Hadron Collider (LHC) as a useful addition to the Higgs search, as well as a motivation to improve charm tagging. In this paper, we demonstrate this channel already has comparable reach at the Tevatron to several of the other channels measured for the combined analysis, and, with a little work, could be the second most powerful channel in the 140–190 GeV region.

While impressive limits on the Higgs mass have been set using the  $H \rightarrow WW \rightarrow l^+l^-\nu\bar{\nu}$  channel, a search for the Higgs in the  $H \rightarrow l\nu c j$  final state has a number of important attributes. Foremost, the  $H \rightarrow l\nu c j$  final state can be fully reconstructed to provide a Higgs mass peak. The dilepton plus missing energy  $\cancel{E}_T$  search relies on fitting derivative shapes, such as the transverse mass of the dilepton pair  $M_T^{ll}$ . Second, while the absolute size of the backgrounds is higher, we show in Sec. III the signal to background ratio (S/B) for  $H \rightarrow l\nu c j$  is a factor of 2–4 better than for the  $H \rightarrow l^+l^-\cancel{E}_T$  case. Third,  $H \rightarrow l\nu c j$  is sensitive to an independent set of backgrounds, providing a robustness check on the Higgs mass limits. This may be important, as recent loosening of cuts in the existing Tevatron analyses [1] may have reopened a sensitivity to the background due to heavy-quark decays

into isolated leptons [10].

A final advantage of the  $H \rightarrow l\nu c j$  channel over the dilepton+ $\cancel{E}_T$  channel is the ability to make use of additional angular correlations in the final state. The key ingredient to reducing both  $WW$  [2–4] and QCD [10] backgrounds in dilepton+ $\cancel{E}_T$  comes about because in a spin-0 Higgs boson decay to  $WW$ , the spins of the  $W$  bosons are anti-aligned. The pure  $V-A$  structure of  $W$  boson decay causes a strong enhancement of the cross section when the charged leptons are aligned. There is also an enhanced probability that the neutrinos align, as seen in Fig. 1, but this information is lost as the neutrinos are unobservable.

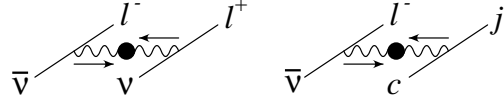


FIG. 1: Angular correlation between leptons in (left)  $H \rightarrow W^-W^+ \rightarrow l^-\bar{\nu}l^+\nu$  and (right)  $H \rightarrow W^-W^+ \rightarrow l^-\bar{\nu}c j$  due to the anti-alignment of  $W$  boson spins in Higgs boson decay.

In Ref. [9] we demonstrated that charm tagging can be used to uniquely identify the correlations between all particles in the final state. In Fig. 1 we see one of the neutrinos of the  $H \rightarrow l^+l^-\nu\bar{\nu}$  channel is replaced by a charm quark. This allows us to make use of both a strong correlation between the charged lepton and the light-quark jet, and between the charmed jet and the neutrino in the event. Despite the fact that the neutrino appears as missing energy, we examine cases where it comes from an on-shell  $W$  decay, and can reconstruct its four-momentum up to a two-fold ambiguity in rapidity.

We have motivated the  $H \rightarrow l\nu c j$  channel as complementary to dileptons+ $\cancel{E}_T$ . In Sec. II we focus on our simulation of the  $l\nu c j$  signal and backgrounds. There we stress the equivalence of our both our modeling of charm tagging and jet energy corrections to existing Tevatron algorithms. We also describe a parametrization of the tagging efficiencies and fake rates we use to predict what benefits could be derived from an increase in charm ac-

\*Electronic address: Zack.Sullivan@IIT.edu

ceptance. In Sec. III we optimize our cuts in three regions, corresponding to whether the  $W$  bosons are off-shell, nearly on-shell, or on-shell, and present the Higgs mass reach. We conclude in Sec. IV by placing our predictions for Higgs mass reach as a function of different charm tagging efficiencies in the context of existing measurements from the Fermilab Tevatron.

## II. JET ENERGY SCALE CORRECTIONS, CHARM TAGGING, AND OTHER SIMULATION DETAILS

Our simulation of signals and backgrounds closely follows our analysis of  $H \rightarrow l\nu c j$  at the LHC [9], with a few improvements for jet energy scales. In order to retain all angular correlations, we generate events at a  $\sqrt{s} = 1.96$  TeV  $p\bar{p}$  collider using MadEvent 4.4 [11] and CTEQ6L1 parton distribution functions (PDFs) [12]. We shower the events with PYTHIA 6.4 [13] and use the PGS 4 [14] detector simulation to reconstruct leptons and jets. Angular correlations in the Higgs signal tend to force the lepton and leading non-tagged jet to be close in phase space. Hence, we reconstruct jets using the PGS jet cone algorithm with a cone size of 0.4. Missing transverse energy  $\cancel{E}_T$  is reconstructed from the calorimeter and corrected for muons. Charm tagging efficiencies and fake rates in PGS are replaced with the ones described below.

In accordance with the experimental analyses, soft jets reconstructed by PGS require large jet energy scale (JES) corrections. The same angular corrections that lead to soft leptons in  $H \rightarrow l^+l^- \cancel{E}_T$  studies, lead to soft jets in our study. Hence, to correct for underestimated gauge and Higgs boson masses in our analysis we calculate a jet energy scale correction as a function of the transverse energy  $E_T$  of the jet.

We derive the JES correction by fitting the shift in the energy between the leading parton generated by  $Zj \rightarrow e^+e^-j$  in MadEvent and the leading jet reconstructed by PGS using a cone size of 0.4. In Fig. 2 we show the data for this extracted jet energy correction with statistical errors, and the best fit curve to this data. The correction is large for low energy jets, and is numerically almost identical to the CDF jet energy correction [15]. We confirm that by applying our JES correction, the Higgs,  $W$ , and  $Z$  gauge boson mass peaks are reconstructed to their correct central values. After we apply the JES correction to the raw PGS output, the following acceptance cuts are used to define jets and leptons:

$$E_T^j > 20 \text{ GeV}, |\eta_j| < 2.0; p_T^l > 20 \text{ GeV}, |\eta_l| < 2.0. \quad (1)$$

In contrast to the main dilepton+ $\cancel{E}_T$  studies, we allow an additional jet to be in the event — consistent with the effects of next-to-leading order (NLO) radiation. We normalize our cross sections to the NLO cross sections obtained after acceptance cuts applied in MCFM 5.8 [16] using CTEQ 6.5 PDFs [17]. Effective  $K$ -factors after cuts are shown in Table I.

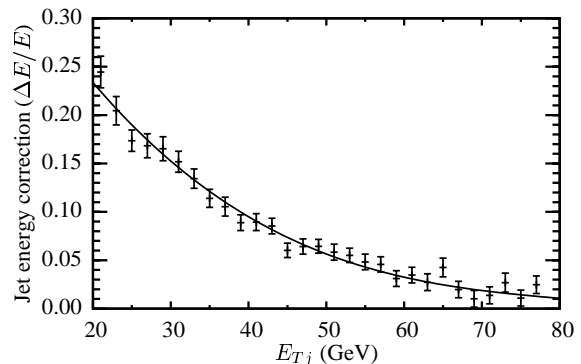


FIG. 2: Jet energy scale correction as a function of the jet transverse energy  $E_{Tj}$ .

TABLE I: Next-to-leading order  $K$ -factors (after acceptance cuts) for the signal and backgrounds.

Signal	$Wcj$	$WW$	$t\bar{t}$	$Wbj$	$t(s)\text{-chan.}$ single top	$Wc\bar{c}$	$Wb\bar{b}$	$Wjj$
2.19	1.39	1.32	1.2	1.59	0.96(1.52)	1.59	1.59	1.39

The key to the measurement of the Higgs boson in the  $H \rightarrow l\nu c j$  channel is charm tagging. More specifically, the key is charm *acceptance*, as the dominant background will turn out to be direct  $Wcj$  production. Hence, we explore several possible tagging and fake rate efficiencies in order to map out the possible spectrum of results.

We model the transverse energy  $E_T$  dependence of the tagging efficiencies utilizing existing impact parameter  $b$ -tagging algorithms based on Tevatron Run I codes [18] (as appear in PGS 3.2 and earlier), and Run II (as appear in PGS 4) [14]. Our main results use rescaled Run I-like charm and bottom tagging efficiencies of the form

$$\epsilon_c^1 = k_c \times 0.2 \tanh\left(\frac{E_{Tj}}{42.08 \text{ GeV}}\right),$$

$$\epsilon_b = \min\left[1.0, k_b \times 0.6 \tanh\left(\frac{E_{Tb}}{36.05 \text{ GeV}}\right)\right], \quad (2)$$

where  $k_c = 1$ ,  $k_b = 1$  correspond to current tagging efficiencies. This heavy-flavor tagging algorithm is predominantly a fit to distributions of events in impact parameter vs. track invariant mass [19], and has room for improvements to acceptance by varying the reconstruction cuts. We scale  $k_b = (k_c + 3)/4$  to model overall increases in heavy flavor acceptance. Eventually, 100% of  $b$  jets will be retained as background, but this is an advantage, as we will want to veto events with two heavy-flavor tags. We also assume a constant light jet fake rate  $\epsilon_j = 1\% \times 10^{(k_c-4)/5}$ . The default choices here are consistent with the CDF Run II measurement of  $Wc$  [20], whose kinematics are similar to ours.

As in Ref. [9], we have reproduced all results using a Run II-like algorithm  $\epsilon_c^2$  from PGS 4. The  $E_T$  dependence of the charm tagging efficiencies for  $\epsilon_c^1$  and  $\epsilon_c^2$  are

shown in Fig. 3. Despite the different  $E_T$  dependence, we find exactly the same significances after cuts. Over the kinematic range of the signal charm jets, the charm acceptance is currently  $\sim 12\%$  for both algorithms; and so we present the full details using  $\epsilon_c^1$ . It is likely that modern neural network based tagging algorithms could improve both the acceptance and purity of the charm signal; but we stress again, that the acceptance is the key to this analysis. In Sec. III we provide a complete list of backgrounds, and our predictions can be trivially rescaled to the final results.

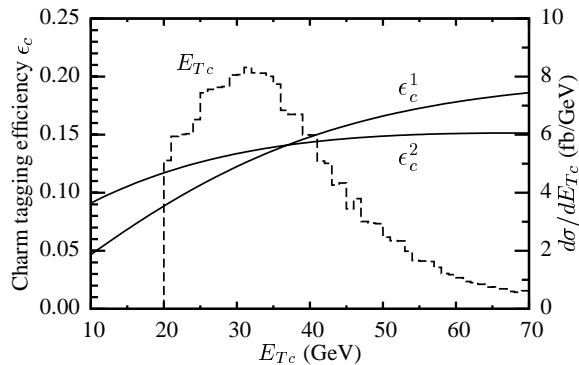


FIG. 3: Charm tagging efficiency curves and characteristic charm jet energy,  $E_{Tc}$ , from  $H \rightarrow WW \rightarrow lvcj$  decay.  $\epsilon_c^1(\epsilon_c^2)$  are existing Tevatron Run I(II)-like algorithms.

### III. ANALYSIS AND MASS REACH FOR $H \rightarrow lvcj$ AT THE TEVATRON

The initial sample for this analysis contains exactly one isolated lepton (electron or muon), two or three jets with exactly one charm tag, and missing transverse energy  $\cancel{E}_T > 15$  GeV. The standard model backgrounds for the  $lcj + \cancel{E}_T$  final state include  $Wcj$ ,  $Wbj$ ,  $Wjj$ ,  $Wc\bar{c}$ ,  $Wb\bar{b}$ ,  $W^+W^-$ ,  $t$ - and  $s$ -channel single top, and  $t\bar{t}$ . By restricting the number of jets to two or three, we reduce significantly the  $t\bar{t}$  background. Charm tagging substantially reduces the  $Wjj$  background, leaving  $Wcj$  as the most important background at most levels of cuts.

Unlike at the LHC, where the  $Wcj$  is the overwhelming dominant background for any charm acceptance, the  $Wb\bar{b}$ ,  $Wbj$ , and  $Wcc$  backgrounds are important at the current low charm-tagging efficiency. Hence,  $S/B$  of this channel at the Tevatron is not as independent of the charm tagging efficiency as that at the LHC. This is evident in Fig. 4, where we show the number of events expected for the signal and each background as a function of  $k_c$ . Nevertheless, the direct  $Wcj$  background scales with the signal, and so our analysis concentrates mostly on reducing its effects.

We optimize our cuts in the three different Higgs mass regions  $m_H < 160$  GeV,  $160 \leq m_H < 170$  GeV, and  $m_H \geq 170$  GeV. For each of these regions the sequence

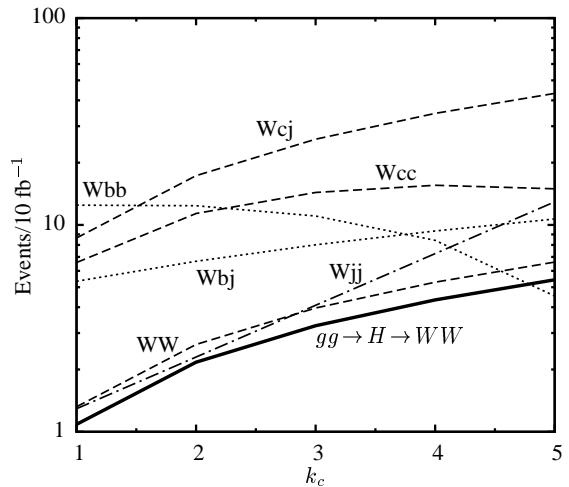


FIG. 4: Number of events in  $10 \text{ fb}^{-1}$  at a 1.96 TeV Tevatron for the  $H \rightarrow lvcj$  signal (solid), and backgrounds from processes with charm jets (dashed), bottom jets (dotted), and light jets (dot-dashed).

of cuts is similar, however the strengths of the cuts are slightly different so as to emphasize the optimal reach at  $m_H = 150$  GeV and  $m_H = 180$  GeV — outside the current Tevatron limits. To compare the Tevatron reach in the  $H \rightarrow lcj + \cancel{E}_T$  channel with the dilepton and other measured channels, we also optimize a search for  $m_H = 165$  GeV.

As  $Wcj$  is the most problematic background, we tune most cuts to reduce its contribution. In the region  $m_H < 160$  GeV we optimize our cuts for  $m_H = 150$  GeV, which are shown in Tab. II. To be concrete, all numbers are presented for  $k_c = 4$ , but we present results for all charm tagging efficiencies below. In this region, at least one of the  $W$  gauge bosons is off-shell, and the signal is typically softer than in the higher mass regions. Therefore, we can impose tight cuts on the upper bounds of  $\cancel{E}_T$ , the charm jet transverse energy  $E_{Tc}$ , and lepton transverse momentum  $p_{Tl}$ . These three cuts reduce the  $Wjj$  oriented backgrounds by a factor of 3, and nearly eliminate  $t\bar{t}$ .

The backgrounds that are independent of charm tagging —  $Wb\bar{b}$ ,  $Wbj$ ,  $t\bar{t}$ , and single top — can be reduced significantly by using the angular correlations between the final state particles. The simplest angular cuts, are those similar to that of  $\Delta\phi_{ll}$  in the leptonic channel, where we cut on  $\cos\theta_{jl}$  the angle between the lepton  $l$  and *leading* non-tagged jet  $j$  in the lab frame. In addition, we know that the directions of the neutrino and  $c$ -jet are correlated. Therefore we can also make a cut  $\cos\theta_{c\nu}$ . In the low Higgs mass region, off-shell  $W$  bosons have weak angular correlations between the jets and leptons. Hence, we make weaker cuts on these angles and on the invariant mass of the jet charm system than for heavier Higgs masses.

In order to reconstruct a Higgs mass peak, we reconstruct the neutrino four-momentum  $p_\nu$  by fitting the lep-

TABLE II: Number of signal ( $H \rightarrow l\nu c j$ ) and background events per  $10 \text{ fb}^{-1}$  of data for  $m_H = 150 \text{ GeV}$  with  $k_c = 4$ .

Cuts	Signal	$Wc j$	$WW$	$t\bar{t}$	$Wb j$	Single top	$Wc\bar{c}$	$Wb\bar{b}$	$Wj j$
1 $l$ , 2 or 3 jets w/ 1 $c$ tag	12	1434	162	31	252	461	442	334	816
$15 \text{ GeV} < \cancel{E}_T < 50 \text{ GeV}$	11	1134	104	8.5	189	258	314	235	464
$E_{Tc} < 65 \text{ GeV}$	9.6	716	67	3.5	132	113	209	160	150
$p_{Tl} < 60 \text{ GeV}$	8.0	354	39	1.8	75	57	118	88	76
$\cos \theta_{jl} > -0.2$	5.9	185	19	0.9	44	33	67	49	43
$\cos \theta_{c\nu} > -0.8$	5.7	172	17	0.8	40	30	60	44	40
$M_{jc} < 100 \text{ GeV}$	5.4	148	17	0.5	33	20	52	40	32
$120 \text{ GeV} \leq M_{l\nu c j} \leq 200 \text{ GeV}$	5.3	144	17	0.5	32	19	50	39	31

ton and  $\cancel{E}_T$  to an on-shell  $W$  boson mass. We take the smallest absolute rapidity  $|\eta_\nu|$  solution to complete the fit. We finish the low-mass Higgs search by placing a cut on the  $M_{l\nu c j}$  invariant mass.

In the region  $m_H \geq 160 \text{ GeV}$  both  $W$  gauge bosons are on-shell. This condition lends itself to slightly different optimizations, as the objects in the final state have more energy on average. In the region  $160 \leq m_H < 170 \text{ GeV}$ , shown in Tab. III, we loosen the upper cut on the  $\cancel{E}_T$ . However, the on-shell condition strengthens the angular correlations. We use this to tighten cuts on  $\cos \theta_{jl}$  and  $\cos \theta_{c\nu}$ .

In addition to the low-mass cuts used in Tab. II, once we are above  $WW$  threshold, the *leading* non-tagged jet  $j$  and the  $c$ -jet have a large opening angle, which allows us to impose a cut on  $\cos \theta_{jc}$ . We also impose a weak  $W$  mass reconstruction cut on  $M_{jc}$ . After Higgs mass reconstruction, the signal to background ratio  $S/B \sim 1/18$  for the 165 GeV Higgs boson in Tab. III, where  $k_c = 4$ . The  $S/B$  is  $1/40$  with current charm acceptance ( $k_c = 1$ ), and is a factor of 2 better than the 0-jet dilepton channel [5].

For masses above 170 GeV, we optimize the cuts for  $m_H = 180 \text{ GeV}$ . As the objects in the events become harder, we loosen the upper limit on  $\cancel{E}_T$ ,  $E_{Tc}$ , and  $p_{Tl}$ . However, we again compensate by tightening the cuts on the angular correlations. The results are shown in Tab. IV.

In Tabs. II–IV we present the detailed effects of cuts level-by-level for 150, 165, and 180 GeV Higgs bosons, and assuming one experiment that collects  $10 \text{ fb}^{-1}$  of integrated luminosity. The CDF and DØ experiments have made a strong effort to combine their Higgs mass-limit analyses in order to improve their reach. In Fig. 5, we scan masses from 140–190 GeV, and compare the 95% exclusion reach of the  $H \rightarrow WW \rightarrow l\nu c j$  channel using  $8.6 \text{ fb}^{-1}$  per experiment to the current preliminary combined Tevatron limits [1]. We demonstrate the importance of the charm acceptance, by presenting separate curves for current charm tagging acceptance  $k_c = 1$  through a best case acceptance of  $\sim 48\%$  ( $k_c = 4$ ). This channel alone can already reach 8.7 times the standard model cross section at 165 GeV current charm tagging, and could reach 3.2 times the standard model cross section if  $k_c = 4$ .

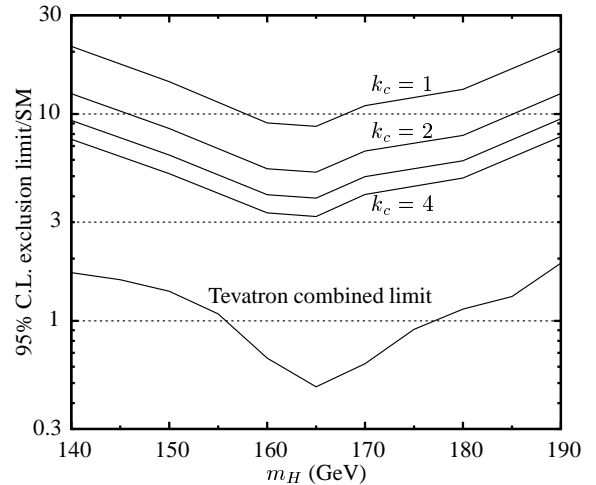


FIG. 5: Expected 95% confidence level (C.L.) exclusion limit on the ratio of the cross-section to that of the standard model (SM) for various charm tagging efficiencies vs. Higgs mass. Also shown is the preliminary combined CDF and DØ analysis including all channels at the Tevatron [1].

#### IV. CONCLUSIONS

A search for the Higgs boson in the channel  $H \rightarrow l\nu c j$  could provide significant additional information to the Fermilab Tevatron Higgs mass exclusion limits. While this channel cannot compete with dileptons+ $\cancel{E}_T$  in absolute rate, it has several strengths in combination with other measurements. The strongest features are that the Higgs mass is completely reconstructable, and the signal to background  $S/B$  is roughly a factor of 2–3.5 better than dileptons+ $\cancel{E}_T$  [5].

To emphasize the complementary nature of this channel, we compare  $H \rightarrow l\nu c j$  to several other channels already studied at the Tevatron. While  $H \rightarrow lc j \cancel{E}_T$  is only sensitive to about 9 times the standard model cross section at current charm acceptances, this is better than several channels in the combined fits. Recent measurements of  $H \rightarrow ZZ \rightarrow l^+ l^- l^+ l^-$  and  $t\bar{t}H$  are sensitive only to cross sections 40–60 times the standard model cross section [7, 8]. In Fig. 6, we show the 95% confidence level exclusion limits from several measurements [1, 6]. If charm tagging acceptance could be improved a factor of 2 ( $\epsilon_c \sim 24\%$ ),  $H \rightarrow lc j \cancel{E}_T$  would have compara-

TABLE III: Number of signal ( $H \rightarrow l\nu c j$ ) and background events per  $10 \text{ fb}^{-1}$  of data for  $m_H = 165 \text{ GeV}$  with  $k_c = 4$ .

Cuts	Signal	$Wc j$	$WW$	$t\bar{t}$	$Wb j$	Single top	$Wc\bar{c}$	$Wb\bar{b}$	$Wj j$
1 $l$ , 2 or 3 jets w/ 1 $c$ tag	16	1434	162	31	252	461	442	334	816
$15 \text{ GeV} < \cancel{E}_T < 55 \text{ GeV}$	15	1209	110	11	193	330	579	218	520
$E_{Tc} < 65 \text{ GeV}$	13	721	84	4.9	144	165	410	160	157
$p_{Tl} < 60 \text{ GeV}$	11	361	51	2.5	83	92	232	86	78
$\cos \theta_{jl} > -0.3$	6.1	108	14	0.8	30	32	72	29	25
$\cos \theta_{c\nu} > -0.6$	5.6	86	10	0.5	23	23	49	22	18
$\cos \theta_{jc} < 0.8$	5.2	68	8.2	0.3	19	14	41	19	14
$50 < M_{jc} < 100 \text{ GeV}$	4.3	35	5.3	0.1	9.4	5.6	16	8.4	7.3
$135 \text{ GeV} \leq M_{l\nu c j} \leq 195 \text{ GeV}$	4.1	33	5.3	8.6	4.4	0.9	14	8.2	6.9

TABLE IV: Number of signal ( $H \rightarrow l\nu c j$ ) and background events per  $10 \text{ fb}^{-1}$  of data for  $m_H = 180 \text{ GeV}$  with  $k_c = 4$ .

Cuts	Signal	$Wc j$	$WW$	$t\bar{t}$	$Wb j$	Single top	$Wc\bar{c}$	$Wb\bar{b}$	$Wj j$
1 $l$ , 2 or 3 jets w/ 1 $c$ tag	14	1434	162	31	252	461	442	334	816
$15 \text{ GeV} < \cancel{E}_T < 70 \text{ GeV}$	14	1351	140	15	235	408	399	298	638
$E_{Tc} < 80 \text{ GeV}$	12	969	105	8.9	191	261	310	234	298
$p_{Tl} < 75 \text{ GeV}$	11	710	81	6.1	139	203	232	173	204
$\cos \theta_{jl} > -0.3$	8.4	410	45	3.5	92	143	142	107	125
$\cos \theta_{c\nu} > -0.4$	7.2	296	28	2.4	63	96	92	71	77
$\cos \theta_{jc} < 0.8$	6.8	261	24	2.2	58	86	67	54	68
$50 < M_{jc} < 100 \text{ GeV}$	5.8	158	21	1.0	35	40	34	30	39
$150 \text{ GeV} \leq M_{l\nu c j} \leq 210 \text{ GeV}$	4.9	118	16	0.6	25	28	23	22	29

ble reach to  $WH \rightarrow WWW$ , currently the second most powerful individual channel.

As data taking at the Fermilab Tevatron comes to a close, the CDF and DØ Collaborations will work to produce strong combined limits on a standard model-like Higgs boson mass. For these final searches, we recommend adding the channel  $H \rightarrow l\nu c j$  to the list of measurements used in the combinations. Not only is this channel interesting by itself, but its sensitivity to completely independent backgrounds will enhance the robustness of

the limits.

### Acknowledgments

This work is supported by the U. S. Department of Energy under Contract Nos. DE-FG02-94ER40840 and DE-FG02-96ER40969.

- 
- [1] Tevatron New Phenomena and Higgs Working Group [CDF and DØ Collaborations], arXiv:1107.5518 [hep-ex].
  - [2] V. D. Barger, G. Bhattacharya, T. Han, and B. A. Kniehl, Phys. Rev. D **43**, 779 (1991).
  - [3] M. Dittmar and H. K. Dreiner, Phys. Rev. D **55**, 167 (1997).
  - [4] T. Han and R. J. Zhang, Phys. Rev. Lett. **82**, 25 (1999).
  - [5] CDF Collaboration, public note 10599.
  - [6] DØ Collaboration, public note 6219-CONF.
  - [7] CDF Collaboration, public note 10573.
  - [8] CDF Collaboration, public note 10574.
  - [9] Arjun Menon and Zack Sullivan, arXiv:1006.1078 [hep-ph].
  - [10] Zack Sullivan and Edmond L. Berger, Phys. Rev. D **74**, 033008 (2006); Phys. Rev. D **82**, 014001 (2010).
  - [11] J. Alwall *et al.*, JHEP **0709**, 028 (2007).
  - [12] J. Pumplin *et al.*, J. High Energy Phys. **0207**, 012 (2002).
  - [13] T. Sjostrand *et al.*, Comput. Phys. Commun. **135**, 238 (2001); T. Sjostrand *et al.*, arXiv:hep-ph/0308153.
  - [14] PGS 4, [physics.ucdavis.edu/~conway/research/software/pgs/pgs4](http://physics.ucdavis.edu/~conway/research/software/pgs/pgs4).
  - [15] A. Bhatti *et al.* (CDF Collaboration), Nucl. Instrum. Meth. **A566**, 375-412 (2006).
  - [16] J. M. Campbell and R. K. Ellis, Phys. Rev. D **60**, 113006 (1999).
  - [17] W.K. Tung *et al.*, J. High Energy Phys. **0702**, 053 (2007).
  - [18] M. Carena *et al.* (Higgs Working Group Collaboration), in *Physics at Run II: the Supersymmetry/Higgs Workshop*, Fermilab, 1998, edited by M. Carena and J. Lykken (Fermilab, Batavia, 2002), p. 424.
  - [19] Barry Wicklund, private communication.
  - [20] T. Aaltonen *et al.* (CDF Collaboration), Phys. Rev. Lett. **100**, 091803 (2008).

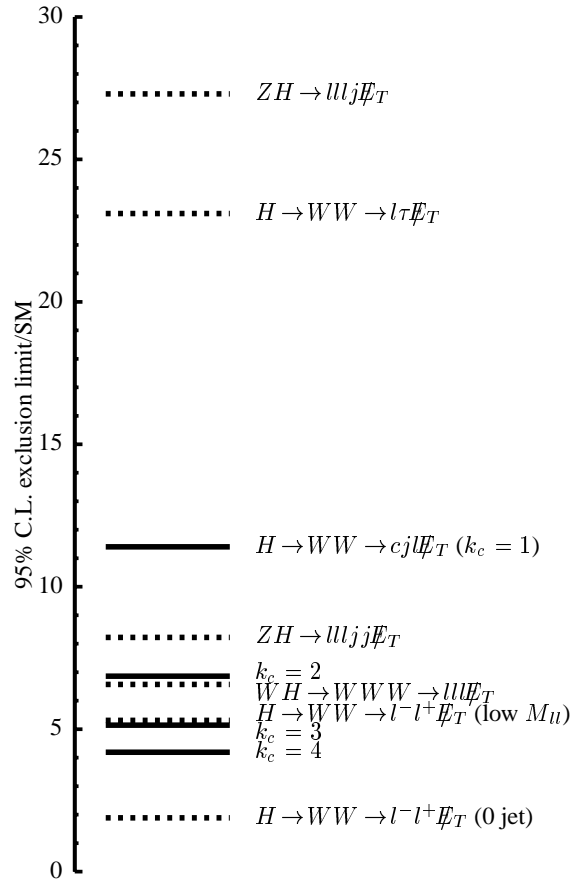


FIG. 6: Comparison of Higgs mass limit reach in  $H \rightarrow cj\cancel{E}_T$  to limits already extracted at the Fermilab Tevatron, for  $m_H = 165$  GeV.